Tree Physiology 29, 483–496
doi:10.1093/treephys/tpn048

The polar auxin transport inhibitor NPA impairs embryo morphology and increases the expression of an auxin efflux facilitator protein PIN during *Picea abies* somatic embryo development

INGER HAKMAN,[1,2] HENRIK HALLBERG[1] and JOAKIM PALOVAARA[1]

[1] *School of Pure and Applied Natural Sciences, University of Kalmar, SE-391 82 Kalmar, Sweden*

[2] *Corresponding author (inger.hakman@hik.se)*

Received October 20, 2008; accepted December 10, 2008; published online January 28, 2009

Summary Auxin and polar auxin transport have been implicated in controlling embryo patterning and development in angiosperms but less is known from the gymnosperms. The aims of this study were to determine at what stages of conifer embryo development auxin and polar auxin transport are the most important for normal development and to analyze the changes in embryos after treatment with the polar auxin inhibitor *N*-1-naphthylphthalamic acid (NPA). For these studies, somatic embryos of Norway spruce (*Picea abies* L. Karst) were used. Growth on medium containing NPA leads to the formation of embryos with poor shoot apical meristem (SAM) and fused cotyledons, and to a pin-formed phenotype of the regenerated plantlets. The effect of NPA on embryo morphology was most severe if embryos were transferred to NPA-containing medium immediately before cotyledon initiation and SAM specification. Indole-3-acetic acid (IAA) was identified by immunolocalization in developing embryos. The highest staining intensity was seen in early staged embryos and then decreased as the embryos matured. No clear IAA-maxima was seen, although the apical parts of embryos, particularly the protoderm, and the suspensor cells appear to accumulate more IAA, as reflected by the staining pattern. The NPA treatment also caused expanded procambium and a broader root apical meristem in embryos, and a significant increase in the expression of a *PIN1*-like gene. Taken together, our results show that, for proper cotyledon initiation, correct auxin transport is needed only during a short period at the transition stage of embryo development, probably involving PIN efflux proteins and that a common mechanism is behind proper cotyledon formation within the species of angiosperms and conifers, despite their cotyledon number which normally differs.

Keywords: conifer, meristem, qRT-PCR.

Introduction

In seed plants, the basic body organization of the sporophyte is established during embryogenesis and is uniform across different species, even if major differences can be seen between the gymnosperms and the angiosperms at their earliest reproductive stages. For instance, in gymnosperms, the female gametophyte serves the dual function of bearing gametes (egg cells within the archegonia) and nourishing the embryo (Singh 1978, Raghavan and Sharma 1995), and a significant feature of the conifer type of embryogenesis is the brief period of free-nuclear divisions before cellularization of the proembryo within the archegonium. Later, during embryo development the embryonal tube cells that are derived from the proximal end of the embryonal mass are added to the suspensor system (Singh 1978). Compared to the model plant *Arabidopsis thaliana* (L.) Heynh., the conifer embryos also show a more irregular division pattern during embryogenesis (Spurr 1949), and a cell corresponding to the hypophysis in *Arabidopsis* (Berleth and Chatfield 2002) cannot be recognized. Despite these differences, the mature embryos of seed plants display the same apical–basal polarity and demarcation of embryonic organs and tissue layers.

The plant hormone auxin (indole-3-acetic acid, IAA) is thought to be a key signal molecule in providing positional information within the embryo, and to be of particular importance during the transition of embryos from globular stage into heart stage in *Arabidopsis* (e.g., reviewed by Jenik and Barton 2005, Weijers and Jürgens 2005, Jenik et al. 2007). Experiments with auxin and 2,3,5-tri-iodobenzoic acid (TIBA), an inhibitor of polar auxin transport, on cut carrot somatic embryos that were either back-grafted or left separated, suggested that the apical part of the embryo inhibits the basal part growth and that this inhibition is controlled by the polar auxin transport or the accumulation of auxin at the root end or both (Schiavone 1988). Further evidence of the importance for polar auxin transport to establish the bilateral symmetry of angiosperm embryos came from the work of Liu et al. (1993) on *Brassica juncea* (L.) Czern. embryos cultured in the presence of polar auxin transport inhibitors. Most importantly, they observed the similarity between their most severe phenotype with that of the *Arabidopsis pin-formed1* mutant

(*pin1*). The *pin1* mutant has reduced polar auxin transport (Okada et al. 1991), and it shows several morphological abnormalities (Gälweiler et al. 1998, Aida et al. 2002, Benková et al. 2003, Furutani et al. 2004). Also, the same mutant phenotype was seen in wild-type *Arabidopsis* plants that are cultured in the presence of auxin polar transport inhibitors (Okada et al. 1991).

Controlled, directional distributions of auxin seem to be set up by an active cell-to-cell auxin flow throughout the plant body that involves transport facilitators of both influx proteins of the AUX/LAX family and efflux-facilitating proteins of the PIN-FORMED (PIN) family, and the ABC-type transporters of the ABCB/P-glycoprotein/multidrug resistance family (Gälweiler et al. 1998, Swarup et al. 2000, Petrásek et al. 2006, Titapiwatanakun and Murphy 2008, Verrier et al. 2008). Several lines of evidence indicate that different expression of transporters of the PIN family and their polar localization within the cells are required for a dynamic auxin gradient with polar auxin transport between cells. Recently applied computer models also support this idea (see e.g., review by Kramer 2008), with the global PIN topology being the most important for robust auxin gradients (Grieneisen et al. 2007).

In the course of the discovery of how auxin is distributed in various organs and tissues, and how its accumulation changes during various developmental processes, several techniques have been used, including immunolocalization with an anti-auxin antibody, monitoring radioactively labeled auxin, direct measurement of endogenous auxin and observation of the activity of auxin-responsive marker genes (e.g., Tanaka et al. 2006). During *Arabidopsis* embryo development, two fluxes of auxin are predicted. Before the globular stage, auxin is assumed to be channeled upward to the embryo from the suspensor cells, as is also reflected by PIN7 localization. At the globular stage, PIN1 and PIN7 become relocalized, and together with PIN4 establish an apical-to-basal auxin flux with an auxin accumulation in the hypophysis that triggers root pole specification (Steinmann et al. 1999, Friml et al. 2003, reviewed by Nawy et al. 2008). Additional auxin gradients are seen in incipient cotyledon primordia that are associated with PIN1 localization (Benková et al. 2003, Friml et al. 2003). In addition to PINs, both PGP1 (ABCB1) and PGP19 (ABCB19/ MDR1) function in a transport mechanism that contributes to the patterning process during *Arabidopsis* embryo development (Mravec et al. 2008).

Although *pin* mutants show strong defects in early embryos, they recover at later stages, which suggest functional redundancy among *PIN* genes (Benková et al. 2003). In addition, when auxin biosynthesis rates were manipulated in *Arabidopsis* embryos, a polar auxin transport activity apparently buffered the normal distribution of auxin within the embryo suggesting a compensatory mechanism for buffering auxin gradients in the embryo, with PIN1 and PIN4 being the most important (Weijers et al. 2005).

Due to their inaccessibility along with other difficulties associated with developmental studies of conifer seed embryos, we use somatic embryogenesis (Hakman et al. 1985) as an experimental system to gain better knowledge about cellular and molecular changes that take place during conifer embryogeny. In a recent study, we analyzed the expression of *WUSCHEL-related homeobox* (*WOX*) family genes during conifer embryo development (Palovaara and Hakman 2008). Different *WOX* genes in *Arabidopsis* have been shown to be expressed in a lineage-specific manner during early embryogenesis (Haecker et al. 2004) and to be involved in axis formation and in the correct expression of *PIN1* (Breuninger et al. 2008). In the present investigation, we have analyzed at what stages during somatic embryo development the inhibition of polar auxin transport with *N*-1-naphthylphthalamic acid (NPA) is most damaging for normal embryo development. We followed structural changes that take place in embryos as well as in the spatial distribution of IAA, as detected by an immunocytochemical approach. Given the importance of PIN proteins in establishing auxin gradients within *Arabidopsis* embryos, a *PIN1*-like homologous gene was cloned (Palovaara et al. unpublished) and its expression pattern was followed during *P. abies* somatic embryo development and also examined in precotyledonary NPA-treated embryos.

Materials and methods

Plant material and somatic embryo culture

One embryogenic cell line of Norway spruce (*P. abies*), designated as 04WV5+h#3, with a high embryo maturation capacity was used in this study. This cell line was initiated and cultured as described recently (Palovaara and Hakman 2008). The embryogenic 'calli', which contained a mixture of early staged embryos, cell aggregates and single cells of diverse form and size were regularly subcultured for continuous proliferation and kept at 25 °C in darkness. For somatic embryo development, small pieces of calli were, with a pair of forceps, carefully spread into a thin layer on top of a filter paper on a maturation medium (MM) (Palovaara and Hakman 2008). Calli and developing somatic embryos of various stages were isolated as previously described (Palovaara and Hakman 2008). Plantlets were regenerated by placing embryos on a plant conversion medium (PCM) containing a modified half-strength Litvay medium (LV-salts, Duchefa, The Netherlands), according to Attree and Fowke (1995).

Seeds of *P. abies* were germinated at 25 °C under a 12-h photoperiod in a growth chamber. Root tips were cut from 2-week-old seedlings, and processed for immunohistochemistry, as described in the following sections.

NPA treatment

Appropriate volumes of a 1 mM stock solution of NPA (OlChemIm, Czech Republic) in dimethyl sulfoxide (DMSO) were added to 20 ml MM within 9-cm Petri

dishes to give the final concentrations of 0.1, 1, 10 and 20 μM, respectively. Equivalent volumes of DMSO were added to all control cultures. Pieces of embryogenic calli, 1 week after last subculture, were transferred to filter papers placed on top of the NPA-containing MM in Petri dishes, as described above for embryo development. The filter papers were, with its developing embryos, then transferred to fresh NPA-containing medium each week during the whole culture period. The development of somatic embryos was followed during 6 weeks. Mature embryos were then isolated and transferred to a PCM that lacked added hormones for another 2 weeks when their growth behavior was again recorded. In another experiment, embryos were first grown on MM for 1, 2, 3 or 4 weeks, before they were transferred to MM containing 10 μM NPA (see Table 3). The cultures were kept at 25 °C in the dark for embryo development and in light for plant conversion. Treatments were made in triplicates and repeated twice. Embryos were fixed for light microscopy and for IAA immunolocalization after various times.

Microscopy and immunohistochemical localization of IAA

Somatic embryo development was followed with an Olympus SZX12 stereomicroscope (Tokyo, Japan) equipped with an Olympus DP10 camera (Tokyo, Japan), and pictures were taken regularly for documentation. Somatic embryos were sampled from Petri dishes at random, except for cultures growing on the highest concentration of NPA/DMSO, in which case only a few embryos had developed. Embryos were embedded in paraffin for structural studies and auxin immunolocalization, as described below. Micrographs were taken with a Zeiss Axiovert 10 inverted microscope (Jena, Germany) equipped with a Leica DFC 320 camera (Wetzlar, Germany). Pictures were further processed using Adobe® Photoshop® CS (San Jose, CA).

Somatic embryos were, for auxin immunolocalization, prefixed in a 3% (w/v) freshly prepared solution of 1-ethyl-3-(3-dimethylaminopropyl)-carbodiimide (EDAC, Sigma) under vacuum for 1 h at 4 °C. They were then post-fixed in FAA (3.7% formaldehyde:50% ethanol:5% glacial acetic acid) under vacuum at 4 °C for 4 h, dehydrated with a graded ethanol series, embedded in paraffin and sectioned into 7-μm slices on a Leitz 1516 rotary microtome (Wetzlar, Germany) and placed on polylysine-coated slides. Dried sections were deparaffinized with xylene and hydrated in an ethanol–water series. For immunolocalization of IAA, an anti-IAA monoclonal antibody (Sigma) raised against carboxyl-linked IAA was used (Leverone et al. 1991, Caruso et al. 1995). Sections were incubated overnight at 10 °C with the primary antibody diluted 1:200, and at room temperature for 4 h with the secondary antibody diluted 1:2000 (AP-conjugated anti-mouse IgG, Promega). The procedure described by Moctezuma (1999) was then followed. Control experiments included sectioned material that had not been prefixed with EDAC, and slides in which either the primary or the secondary antibodies were omitted.

All experiments were repeated with at least three different embryos of each embryo developmental stage and for each treatment.

Before proceeding to the immunolocalization of IAA in somatic embryos, we tested the specificity of the anti-IAA antibody and verified the effectiveness of the method on seedling root tips of *P. abies*. The samples were processed as described above.

Absolute qRT-PCR of PIN expression

Total RNA was extracted as previously described (Palovaara and Hakman 2008) from different staged somatic embryos maturing on MM, and from precotyledonary (stage 2) embryos growing on 1 μM NPA. For cDNA synthesis, 2 μg of total RNA was reverse transcribed with oligo (dT) and random hexamer primers using the iScript™ cDNA synthesis kit (Bio-Rad, Hercules, CA) according to the manufacturer's protocol.

A 140-bp sequence of a potential *PIN1*-orthologous gene (Accession No. FJ031883) was amplified from *P. abies* somatic embryos with a forward primer (5′-CGAAAAA CATAAACAGATGCCCCC-3′) and a backward primer (5′-TCCACCTGAAAGAAACGAGTGC-3′). The primer pair was tested to ensure the amplification of a single discrete band with no primer–dimers using the same optimized conditions as described below for quantitative reverse transcription polymerase chain reaction (qRT-PCR). The resulting product was sequenced by MWG-Biotech (Ebersberg, Germany) to verify the correct gene product, and Invitrogen (Paisley, UK) synthesized the primers.

Quantitative RT-PCRs were performed with a MiniOpticon Real-Time PCR Detection System (Bio-Rad, Hercules, CA). The reactions were done in a 25 μl volume containing 12.5 μl iQ SYBR Green Supermix (Bio-Rad), 0.4 μM of both primers and 2 μl of cDNA template. The thermal cycling conditions were as follows: 3 min at 95 °C, followed by 40 cycles of 10 s at 95 °C, 10 s at 58 °C and 10 s at 72 °C. Expression levels were determined as the number of cycles needed for the amplification to reach a threshold fixed in the exponential phase of the PCR (C_t) (Walker 2002). Absolute quantification of *PIN1*-like copy number in each cDNA sample was determined using a standard curve and normalized against micrograms total RNA as previously described (Palovaara and Hakman 2008).

All samples and the standard curve were run in triplicates ($n = 3$) and three assays were performed using three independent samples of each tissue collected. Negative (distilled water) and no-template (total RNA) controls were included in each run. After normalization, average values and standard errors of gene copy numbers were calculated using data from triplicate assays. Statistically significant differences were evaluated by one-way analysis of variance (ANOVA), followed by post hoc Tukey's HSD comparisons and

Student's t test using STATISTICA Version 7.1 (StatSoft, Inc.). Differences of $P < 0.05$ were regarded as significant.

Results

Cell line characterization and somatic embryo development

During proliferative growth on the maintenance medium, which contained both auxin and cytokinin, early staged somatic embryos were continuously produced together with aggregates of small rounded cells and more elongated all intermingled and forming a white-to-translucent type of cell mass (callus) (Figure 1A). Somatic embryos of this early stage (here denoted as stage 1) had a small embryo proper, composed of small cells with dense cytoplasm, that was subtended by highly elongated cells forming a suspensor-like structure (Figures 1B and 5D). Such embryos were continuously formed in calli on the proliferation/maintenance medium but never developed beyond this stage. After transfer to the MM, the callus continued for some time to proliferate, although not as fast, forming a dense mat of cells. New embryos were formed within the callus at the same time as embryos continued to develop. During the first 2 weeks on MM, early staged (stage 1) somatic embryos increased both in number and in size (Figure 1C). Both the embryo proper and the suspensor became larger and well structured (Figure 3A). Next, the embryo proper increased further in size and became more opaque and club-like in shape with a smooth and glistening surface (stage 2) (Figure 1D). After about 4 weeks on MM, cotyledons, although still small, were seen to develop as a circlet at the embryo apex (stage 3) (Figure 1E and F). Thereafter, the cotyledons increased in size at the same time as the embryos elongated further (Figure 1G and H). Embryos are considered mature at this stage (stage 4), and further growth is usually detained while embryos are kept on MM.

Effect of different concentrations of NPA on the development of somatic embryos

In one experiment, somatic embryos were kept for the whole embryo maturation period on MM containing NPA of different concentrations (Table 1; Figure 2A–C). Cultures grown on MM with 0.1 and 1 μM NPA had during the first 2–3 weeks a growth behavior and morphology similar to that of the control. The effects of NPA on embryo morphology, however, became apparent as the embryos developed further. After 4–5 weeks on the MM, the control embryos initiated cotyledons that were well separated (Figure 1E and F). Many of the embryos growing on 0.1 and 1 μM NPA formed a cup-like structure instead (Figure 2A–C) or, in the more severe cases, they were pin-formed (Figure 2B). Such defects were most severe for embryos growing on 1 μM NPA. Also, the developmental arrest of mature embryos seemed to be less pronounced after NPA treatment, as embryos elongated more and cotyledons were more greenish. Higher concentrations of NPA were harmful and only a few deformed embryos developed on medium with 10 μM NPA and none on medium with 20 μM NPA. Already 1–2 weeks on medium containing such high NPA concentration was damaging to the young developing embryos, as described more thoroughly in the following sections, and only very minor proliferation took place. Some of these harmful effects could probably be ascribed to DMSO, because at least the higher concentration of DMSO also obstructed growth.

The disturbing effect of NPA on proper embryo development, such as was seen for the cotyledon formation, was even more manifest after embryo germination (Table 2A). Embryos that had developed on NPA medium for 6 weeks continued to grow into pin-formed plantlets after an additional 2 weeks on the PCM, with no hormones or NPA added (see figures in Table 2). Plantlets with many well-separated cotyledons were rarely formed from the NPA-treated embryos, whereas such were common in the control cultures. The pin-formed phenotype was more common at higher NPA concentrations.

High concentration of NPA is damaging to early staged embryos

Because the higher NPA concentrations (10 and 20 μM) had such a negative effect on the initial growth of the calli, we followed the fate and the growth behavior of cells and embryos during their first 1–3 weeks on MM with 10 μM NPA, and compared them to cultures kept on MM alone. During the first week of culture, the embryos looked similar, but during the second week of culture they showed quite different morphologies. The embryos growing on MM alone had increased embryo proper with well-structured and united suspensor-like cells (Figure 3A), whereas the embryos on MM medium with 10 μM NPA appeared to disintegrate (Figure 3B and C). It is uncertain if NPA caused a disturbance in directional auxin transport in early embryos that resulted in such severe developmental defects from which they could not later recover, or if this was caused by a more unspecific effect of NPA not related to polar transport of auxin. Also, NPA in combination with the solvent could negatively affect the embryos.

Embryo developmental stages that are most affected by NPA

Next, we wanted to pinpoint at what embryo developmental stages that NPA treatment caused the most aberrant/pin-formed embryos. The embryos were grown on MM alone for various times (1–4 weeks; for culture outline and summary, see Table 3) before being transferred to 10 μM NPA-containing MM, for the embryos to first reach different developmental stages (stages 1–3). Even though 10 μM NPA was found to be detrimental to embryos if they were kept on that high concentration during their whole embryo maturation period (Tables 1 and 3), (i.e., it was particularly the

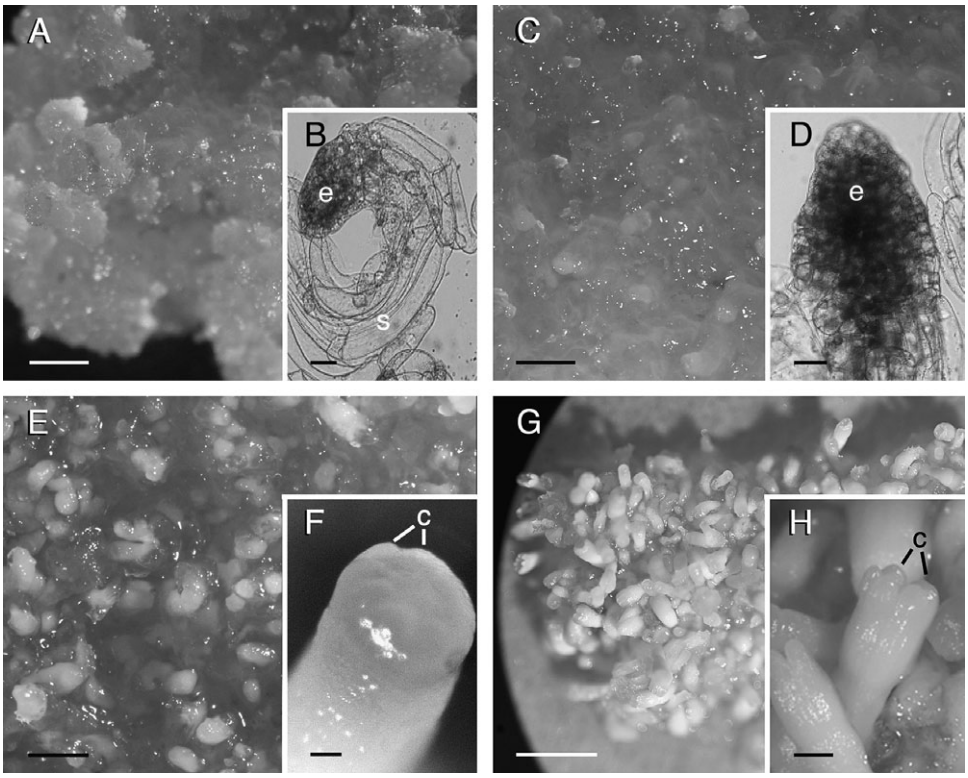

Figure 1. *Picea abies* somatic embryo development: (A and B) stage 1 embryos formed in proliferating cultures maintained on medium containing both auxin and cytokinin; (C and D) stage 2 embryos after 2 weeks on MM; (E and F) stage 3 embryos after 4 weeks on MM; (G and H) stage 4 embryos after 5 weeks on MM. Bars in A, C and E = 1 mm, B and D = 50 μm, F = 100 μm, G = 5 mm and H = 500 μm. c, cotyledon; e, embryo proper; s, suspensor. A color version of this figure is available as Supplementary Data at *Tree Physiology* Online.

earliest staged embryos that were damaged during their first weeks of growth, as described above (Figure 3B and C)), this concentration was chosen because the effect would be more pronounced on the more advanced embryos. Embryos did only develop on the NPA-containing MM if they had first been cultured on MM without NPA for at least 2 weeks before NPA treatment, and the phenotype of the embryos depended entirely on the developmental stage that they had reached before the NPA-treatment (Table 3). The most aberrant phenotype was seen on embryos that were transferred to NPA-containing medium after 2 and 3 weeks on MM, that is, before they had initiated cotyledons (stage 2 embryos). Their morphology was similar to embryos that had been growing on low NPA-concentration during their whole maturation period. Embryos that had already initiated cotyledon, even the tiniest ones, before being transferred to NPA-containing medium, did not show any severe phenotypes, although the mature embryos had cotyledons that appeared slightly thicker and more greenish compared to the control embryos (Figure 2D). Again, the effect of NPA on embryo development was further confirmed by germinating embryos on PCM for 2 weeks (Table 2B).

Structural changes of NPA-treated embryos

Embryos that had been treated with various concentrations of NPA during their whole maturation period, or with 10 μM NPA after first being cultured for 2 weeks on MM without NPA, were embedded and sectioned for the analysis of their anatomy and for the immunolocalization of auxin. Control embryos included both embryos growing on MM alone and embryos growing on MM with DMSO added. The embryos treated with 0.1 and 1 μM NPA were at the early precotyledonary stages, quite similar in structure to that of the control embryos (cf. Figure 4A, C and E). Many of them, particularly if grown on the lower concentration of NPA, had formed a root apical meristem (RAM), with observable columella cells within the root cap (cf. Figure 4A and C), while in others the RAM was more difficult to distinguish (Figure 4E). As embryos matured, the anatomy of the NPA-treated embryos and the control embryos became more dissimilar.

Embryos that matured on MM had a well-organized RAM and many well-separated cotyledons that were connected with procambial cells (Figure 4B). In NPA-treated embryos, irrespective of whether they had been continuously cultured on a low concentration of NPA (Figure 4D, F and G) or transferred to a high concentration of NPA after their second week on MM (Figure 4H), the RAM was much broader and not as well demarcated. Cells closer to the surface in the root area still had the characters of root cap cells, such as they contained large starch grains. No shoot apical meristem (SAM) could be identified with certainty in the NPA-treated embryos and the cotyledons had often fused. Depending on the plane of the section, the cotyledons appeared fused or not (cf. Figures 2C with 4G and H). In the thin sections this created a hollow space at the presumed SAM area. Even if the internal

Table 1. Effect of different NPA concentrations on somatic embryo development.

Culture time (weeks)	Amount of NPA or DMSO added to 20 ml culture medium							
	0 µl	2 µl DMSO	2 µl NPA (0.1 µM)	20 µl DMSO	20 µl NPA (1.0 µM)	200 µl DMSO	200 µl NPA (10 µM)	400 µl DMSO	400 µl NPA (20 µM)
1	+ + + st1–2	+ + + st1–2	+ + + st1–2	+ + + st1–2	+ + + st1–2	+ + + st1–2	+ + few st1–2	+ + few st1–2	+ few st1–2
2	+ + + st2	+ + + st2	+ + + st2	+ + + st2	+ + + st2	+ + + st2	+ + few st2	+ few st2	+ no embryos
3	+ + + st2–3	+ + + st2–3	+ + + st2–3	+ + + st2–3	+ + + st2–3	+ + + st2	+ few st2	+ few embryos	– no embryos
4	+ + + st3	+ + + st3	+ + + st3 some cup	+ + + st3	+ + st3 cup/pin	+ + st2, few st3	+ few st2	+ few embryos	– no embryos
5	+ + + st4	+ + + st4	+ + + st4 some cup	+ + + st4	+ + st4 cup/pin	+ + few st4	+ few st2	+ few embryos	– no embryos

Cultures were kept on 20 ml MM including different concentrations of NPA or an equal volume of DMSO added. The proliferation of the tissue cultures was rated from low to high (+ to + + +) and embryo developmental stages were categorized as stages 1–4 (st1–4). Defected embryo morphologies were characterized as cup-shaped (cup) and pin-formed (pin).

organization was disrupted in the NPA-treated embryos, planes of cell divisions were ordered, resulting in longitudinal files of cells both in the root cap area and in the cortical and procambial areas. Sometimes cells of adjacent cell files were seen to have separated from each other. The procambium in the NPA-treated embryos also appeared more expanded compared to the control embryos and, in the more developed embryos, which also had elongated more than the control embryos, tracheids had already differentiated, both with ring- and scalariform-reticulate thickenings. Highly elongated cells that contained a red-brown substance (inset Figure 4G) were often seen in the more developed NPA-treated embryos, even though such cells were sometimes seen in the DMSO-treated embryos.

Taken together, these experiments indicate that precotyledonary embryos (stage 2) are most sensitive to disordered polar auxin transport; that NPA caused cotyledons to fuse, and in extreme cases caused the entire apical part to grow as a pin-like structure; that SAM was poorly defined, if formed at all; that the RAM often became wider and not so well demarcated and that the procambium became more expanded.

Auxin immunolocalization in developing embryos

To verify the method of immunolocalization, root tips of 2-week-old seedlings were used, as the IAA accumulation pattern in them could be assumed to be comparable with that of the published results from angiosperms (Figure 5A–C). In our study, and with the antibodies we used (produced with the IAA carboxyl group linked to ovalbumin; Leverone et al. 1991), we obtained a blue staining reaction whether or not the tissues were first fixed with EDAC (cf. Figure 5A and B). The EDAC is commonly used to cross-link the carboxyl group of IAA to structural proteins within the plant cell and to create epitope recognition for the IAA monoclonal antibody (Leverone et al. 1991, Avsian-Kretchmer et al. 2002). However, in the control sections, when either the primary or the secondary antibodies were omitted, no stain was ever observed (Figure 5C). This demonstrated that the background color was low and that a color signal depended on the presence of both antibodies. The staining pattern we observed on *P. abies* somatic embryos agrees well with that of *Arabidopsis* embryos treated with the same antibody (Avsian-Kretchmer et al. 2002), despite morphological differences between the embryos of the two species. The immuno-distribution pattern also agrees with that of the photoaffinity labeling agent tritiated 5-azidoindole-3-acetic, an IAA analog, that was used with wheat embryos treated with NPA (Fischer-Iglesias et al. 2001).

The youngest staged embryos had, in general, a much deeper blue stain than the more mature embryos (Figures 5D and 4A–H, respectively). Especially stage 1 embryos, present in the proliferating callus, stained dark blue (Figure 5D; cf. with control in Figure 5E), which perhaps reflect

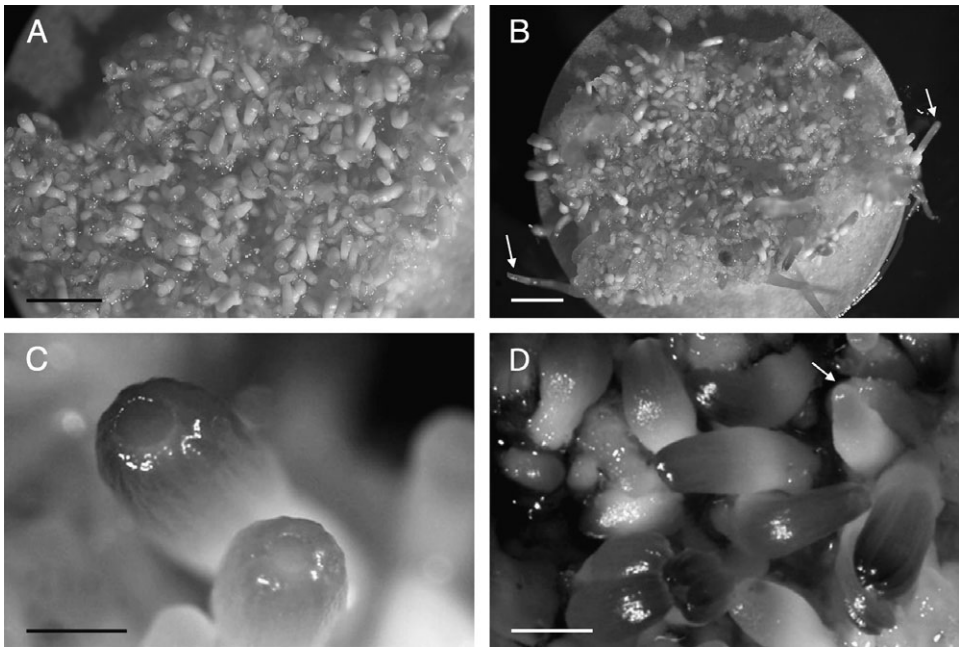

Figure 2. *Picea abies* somatic embryos growing on NPA-containing MM. (A) Somatic embryos were cultured for 5 weeks on MM containing 0.1 μM NPA. (B) Somatic embryos were cultured for 5 weeks on MM containing 1 μM NPA, and note the many pin-formed embryos (arrows). Control embryos grown on MM alone are shown in Figure 1G. (C) Cup-shaped somatic embryos after 5 weeks on MM containing 1 μM NPA. (D) Somatic embryos cultured for 3 weeks on MM and then for 2 weeks on MM containing 10 μM NPA, and note the deep green color of the most advanced embryos and fused cotyledons on young embryo (arrow). Bars in A and B = 5 mm, C = 500 μm and D = 1 mm. A color version of this figure is available as Supplementary Data at *Tree Physiology* Online.

their proliferative growth in the presence of both cytokinin and auxin, even if the medium contained 1-naphthalene acetic acid (NAA) and not IAA. Exogenously applied IAA or its synthetic analog NAA to plant organs often increase the staining signals of auxin without changing the spatial pattern of the signal (Friml et al. 2002, Benková et al. 2003). A clear gradient of stain in embryos could not be detected, even if the embryo proper seemed to stain more in stage 1 embryos (Figure 5D). However, this could also be a consequence of the suspensor cells being highly vacuolated. Also in the precotyledonary stage 2 embryos, the apical parts appeared to stain stronger (Figure 4A, C and E). At this embryo developmental stage, the signal appeared to be highest in the protoderm/epidermis and more so in the control embryos (Figure 4A, inset) than in the NPA-treated embryos (Figure 4C and E, insets). This high staining of the protodermal cell layer also correlates with a high expression of *PIN1*-like in these cells (Palovaara et al. unpublished). As embryos matured they stained less, and most often, the staining reaction in them was highest in the epidermal cells and ground tissue (Figure 4B, D and F–H). Otherwise no definite difference in the staining pattern between the control and the NPA-treated embryos could be recognized. In summary, these results indicate a dynamic change in auxin accumulation in the protodermal/epidermal cell layer during embryo development, and we propose that this is mediated by polar auxin transport, which if disturbed by NPA leads to the deformed pin-formed embryos.

PIN1 expression during somatic embryo development

Next, we analyzed the expression pattern of a *PIN1*-like gene to see how it followed different stages during normal somatic embryo development. An extensive characterization of the gene and its expression in *P. abies* will be published separately, but based on its sequence and expression pattern in somatic embryos we classify the gene as *PIN1*-like (Palovaara et al. unpublished). For the verification of absolute qRT-PCR, a standard curve was generated for the target *PIN1*-like gene, and the effective PCR amplification kinetics was shown by high PCR efficiency per cycle (Table 4A). Assay sensitivities were confirmed by detection limits down to 10 single-stranded DNA molecules and linear quantification ranges between 10 and 10^6 molecules. Intra- and inter-assay variations (expressed as % molecules) of 9.62 (± 3.2) to 16.4, respectively, were determined over the entire quantitative range, showing high precision and reproducibility of the applied assay.

Absolute quantification revealed that the *PIN1*-like gene was expressed specifically during the earliest stages of the somatic embryo development (Table 4B). Expression level was the highest (2.3-fold) in samples taken 6 days after

Table 2. Effect of NPA treatment during embryo maturation on the morphology of regenerated plantlets.

NPA treatment	Number of embryos	Frequency of observed embryo morphology (%)			
A					
NPA concentration (μM)					
0	60	70	0	0	30
0.1	80	30	12	4	54
1.0	60	0	20	40	40
B					
Treatment label (weeks on MM ± NPA)					
2wMM/3wNPA	80	0	17	18	65
3wMM/2wNPA	80	3	26	20	51
4wMM/1wNPA	80	50	14	0	36
		 Normal (many cotyledons)	 Poorly separated cotyledons	 Pin-like (one cotyledon)	 Deformed (curled, swollen or both)

A. Somatic embryos were first grown on MM containing various concentrations of NPA for 6 weeks and then on PCM for 2 weeks. B. Somatic embryos were first grown on MM for 2–4 weeks (w) to reach different stage before transfer to MM including 10 μM NPA for 1–3 weeks. Embryos were then grown on PCM for 2 weeks (see also Table 3 for treatment and growth). A color version of this table is available as Supplementary Data at *Tree Physiology* Online.

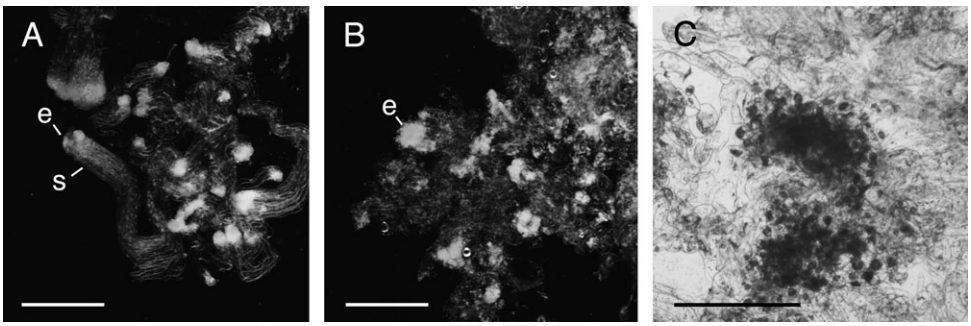

Figure 3. *Picea abies* somatic embryos after 2 weeks on MM. (A) Early staged embryos with well-formed suspensor system (s) and dense embryo proper (e); dark field. (B) Somatic embryos growing in the presence of 10 μM NPA; dark field, and note the disintegrating suspensor cells and embryo proper (e). (C) Disintegrating embryo in the presence of 10 μM NPA; bright field. Bars in A and B = 1 mm and C = 500 μm.

transfer to the MM, which contained mostly stage 1 embryos and also contained stage 2 embryos. The callus growing on maintenance medium contained a variety of cells in addition to stage 1 embryos. In samples that included both stage 2 and 3 embryos together, the absolute expression level was slightly below (1.45-fold) the initial expression level in the callus. In mature embryos (stage 4), the absolute expression increased slightly (1.1-fold) when compared with the callus. Statistical analysis, however, showed only a significant difference in *PIN1*-like expression between the samples containing stage 1 and 2 embryos and the samples containing the rest of the stages.

PIN1 expression increased in NPA-treated somatic embryos

By exogenous application of auxin and auxin transport inhibitors it has been shown that *PIN* expression is modified (Peer et al. 2004, Vieten et al. 2005). Because NPA had such a dramatic effect on the embryo morphology we

Table 3. Effect of NPA treatment on somatic embryos of different developmental stages.

	Number of weeks on MM without NPA □ Number of weeks on MM + 10 μM NPA ■				
Treatment label (weeks [w] on MM ± NPA)	1	2	3	4	5
5wMM/0wNPA	+ + + st 1–2	+ + + st 2	+ + + st 2–3	+ + + st 3	+ + + st 4
4wMM/1wNPA	+ + + st 1–2	+ + + st 2	+ + + st 2–3	+ + + st 3	+ + + st 4
3wMM/2wNPA	+ + + st 1–2	+ + + st 2	+ + + st 2–3	+ + + st 2–3	+ + + st 2–3 few st 4
2wMM/3wNPA	+ + + st 1–2	+ + + st 2	+ + + st 2–3	+ + + st 2–3	+ + + st 2–3 few st 4 (pin/cup)
1wMM/4wNPA	+ + + st 1–2	+ + + st 2	+ + + st 2*	+ + + st 2*	+ + + st 2*
0wMM/5wNPA	+ + st 1–2	+ + st 2*	+ st 2*	+ st 2*	+ st 2*

Somatic embryos were transferred on a weekly basis from MM (□) to MM containing 10 μM NPA (■). The proliferation of the tissue cultures was rated from low to high (+ to + + +), and embryo developmental stages were categorized as stages 1–4 (st1–4). Defected embryo morphologies were characterized as cup-shaped (cup) and pin-formed (pin).
*Damaged; no further growth.

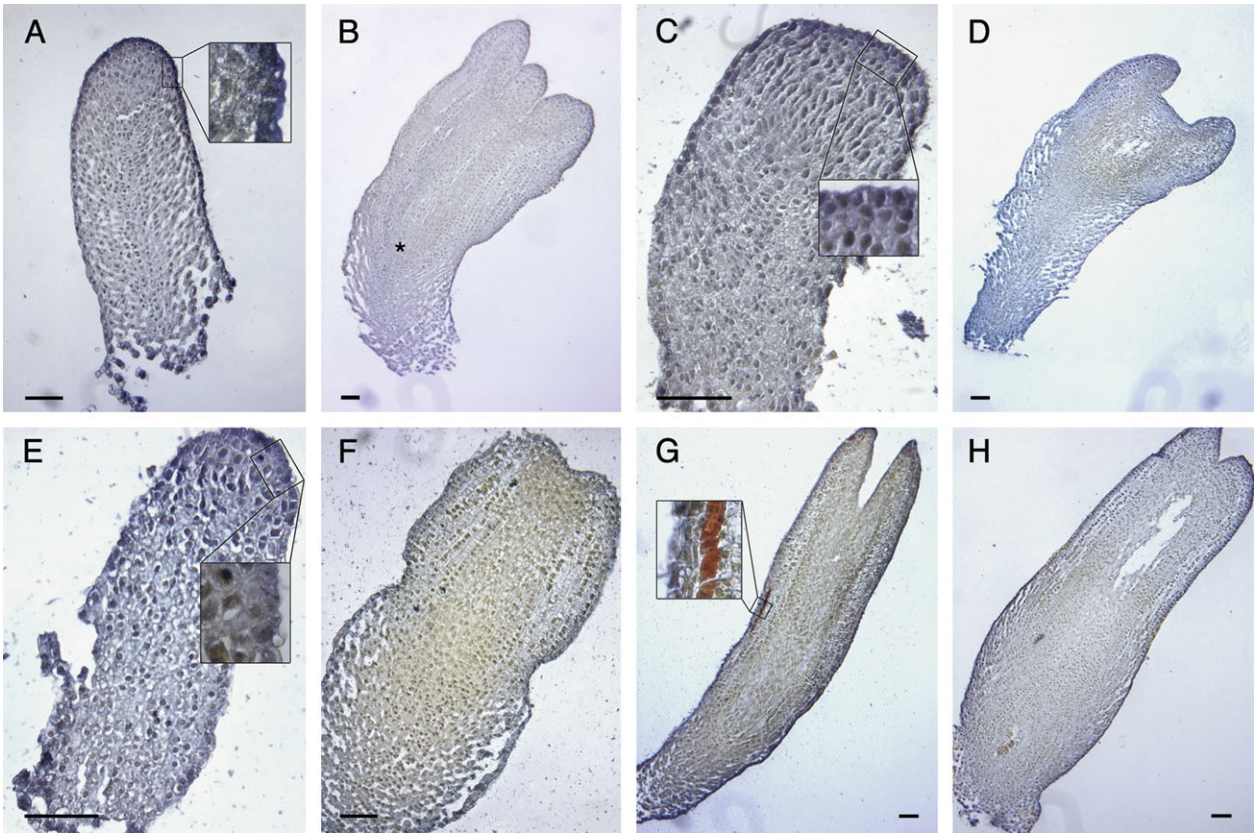

Figure 4. Histological sections of paraffin-embedded *P. abies* somatic embryos developing on MM with different concentrations of NPA. The sections were used for immunolocalization of IAA. All sections were prefixed with EDAC and treated with both primary and secondary antibodies. (A) Stage 2 somatic embryo grown on MM, and note the deeper stain in the protodermal cell layer (inset). (B) Stage 4 somatic embryos grown on MM, and note the well-formed RAM (*). (C) Stage 2 somatic embryo grown on MM with 0.1 μM NPA, and inset shows the protodermal cell layer. (D) Stage 4 somatic embryo grown on MM with 0.1 μM NPA. (E) Stage 2 somatic embryo grown on MM with 1 μM NPA, and inset shows the protodermal cell layer. (F) Cup-shaped stage 4 somatic embryo grown on MM with 1 μM NPA. (G) Pin-formed stage 4 somatic embryo grown on MM with 1 μM NPA, and note the deep staining ideoblasts in cortical layers (inset). (H) Stage 4 somatic embryo grown first on MM without NPA for 2 weeks before transfer to MM with 10 μM NPA. Bars = 100 μm.

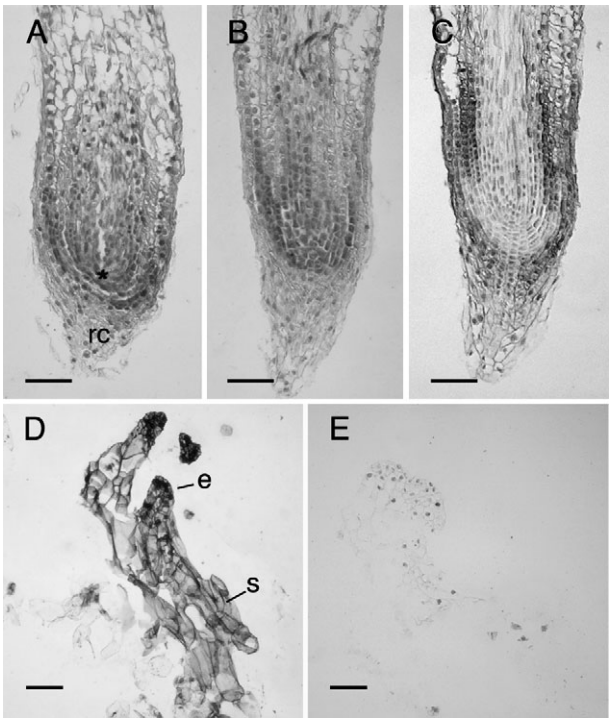

Figure 5. Validation of the method of immunohistochemical localization of IAA in the longitudinal sections of *P. abies* root tips and somatic embryos. (A) Root prefixed with EDAC and treated with both primary and secondary antibodies, and note the RAM (*). (B) Root not prefixed with EDAC. Treated with both primary and secondary antibodies. (C) Root prefixed with EDAC, and primary antibody omitted. (D) Stage 1 somatic embryo prefixed with EDAC. Treated with both primary and secondary antibodies; e, embryo proper and s, suspensor. (E) Stage 1 somatic embryo prefixed with EDAC, and primary antibody omitted. Bars = 100 μm. A color version of this figure is available as Supplementary Data at *Tree Physiology* Online.

examined *PIN1* expression in the NPA-treated (1 μM) somatic embryos. Quantification of the *PIN1*-like gene in the NPA-treated stage 2 embryos revealed a drastic increase in the expression level, significantly higher (13.7-fold) when compared to stage 1 and 2 somatic embryos cultivated on MM alone (Table 4B). This is consistent with the earlier observations in *Arabidopsis* of how the inhibition of auxin transport can modulate *PIN* gene expression in a similar way to that observed in *pin* mutants (Vieten et al. 2005).

Discussion

Drugs that act on polar auxin transport are useful tools when investigating the role of auxin transport in the control of plant development. Of these, NPA, which belongs to a class of structurally related chemicals called phytotropins (Katekar and Geissler 1980), is widely used. Many results indicate that NPA acts by inhibiting auxin efflux from cells, which then, as a consequence, leads to auxin accumulation in treated cells (Petrásek et al. 2003). The mechanism of its inhibitory action is not understood, although studies indicate it to be mediated through NPA-binding protein (NBP) and evidence suggests that there are both a high-affinity site at the plasma membrane associated with the inhibition of auxin transport and a low-affinity NPA-binding site (for review see Petrásek et al. 2003, Titapiwatanakun and Murphy 2008).

NPA damaged the early staged somatic embryos

We observed that the treatment of *P. abies* somatic embryos with the polar auxin transport inhibitor NPA, at 10 μM or higher concentration, during their first 2–3 weeks of maturation growth on the MM was detrimental to them (Table 1; Figure 3), and the embryos appeared as if they disintegrated after a few weeks on the high NPA-containing medium. If this was caused by the general toxicity of NPA to embryos or if it was due to the inhibition of polar auxin transport activity or if NPA has effects on the cells other than for auxin transport is not known. Also, DMSO, which was used as a solvent for NPA, negatively affected the embryos at high concentrations (Table 1). Studies in *Arabidopsis* roots have suggested that the inhibitors of polar auxin transport may interfere with membrane trafficking in a broader sense than just with the continuous cycling of PIN between the plasma membrane and the endosomal compartments (Geldner et al. 2001). This trafficking of PIN1 appears to be actin dependent, and is also sensitive to the vesicle-trafficking inhibitor brefeldin A (BFA), causing accumulation of the PIN1 into the so-called BFA compartments. Such BFA compartments are also seen in young somatic embryos of *P. abies* after exposure to BFA (Gorbatenko and Hakman 1995). However, the concentration of the auxin transport inhibitors required for the inhibition of membrane trafficking was high (Geldner et al. 2001).

The auxin transport inhibitors, TIBA and PBA, were recently shown to have a bundling effect on the actin cytoskeleton, not only in plant cells but also in yeast and mammalian cells (Dhonukshe et al. 2008). The effect of NPA on the actin cytoskeleton, however, seems less clear. In *Arabidopsis* roots NPA was seen to disrupt the actin filaments (Rahman et al. 2007), whereas in cultured tobacco BY2-cells, NPA had no effect on actin (Petrásek et al. 2003). However, in BY2-cells, in which overexpressing mouse talin induced a bundle configuration of actin, the sensitivity to NPA was increased as well as cell division synchrony was disturbed. Both could be restored by polarly transported auxins (Maisch and Nick 2007). In early staged conifer somatic embryos, a fine network of actin filaments is present in the small cells of the embryo proper, whereas prominent cables are formed in the suspensor cells (Hakman et al. 1987), and the effect on them of NPA and other auxin transport inhibitors merits a further investigation.

In addition to PIN, NPA has been shown to interact with members of the P-glycoprotein/ABCB/multidrug resistance

Table 4. Absolute quantification of a *PIN1*-like gene using qRT-PCR. A. Characteristics and validation parameters of *PIN1*-like real-time qRT-PCR in the MiniOpticon Real-Time PCR Detection System. A standard curve with six measuring points, derived from serially diluted *PIN1*-like PCR product, was used. Intra and inter-assay variations were determined over the entire quantitative range and are expressed as percentage molecules. B. Absolute expression of a *PIN1*-like gene in embryos normalized against micrograms total RNA during somatic embryo development and in NPA-treated stage 2 somatic embryos. When comparing developing somatic embryos, mean values are only statistically significantly different ($P < 0.05$) between stages 1–2 and stages 1 (in callus), 2–3 and 4 as evaluated by ANOVA followed by Tukey's HSD. In addition, mean values are statistically significantly different ($P < 0.05$) when comparing untreated stages 1–2 embryos with NPA-treated stage 2 embryos as evaluated by Student's *t* test.

A

	PIN1-like
PCR efficiency	1.93
Detection limit	8 molecules
Quantification limit	83 molecules
Quantification range (test linearity)	83–8.3 × 10^6 molecules ($r = 0.999$)
Intra-assay variation	9.62 ± 2 ($n = 4$)
Inter-assay variation	16.4 ($n = 4$)

B

Development stages	Copy number (×10^4)/µg total RNA[a]	SEM[b]
Stage 1 (in callus)	3.710	0.96
Stage 1–2	8.450	0.85
Stage 2–3	2.570	0.64
Stage 4	4.190	0.79
NPA-treated stage 2	118.2	16.9

[a] Mean of triplicate assays.
[b] Standard error of mean.

family in *Arabidopsis* that are also identified as auxin transporters (Noh et al. 2001, Murphy et al. 2002, Bailly et al. 2008, Nagashima et al. 2008), and recent studies suggest that the auxin efflux activities of the PINs are modified by their association with PGP19/ABCB19 (Blakeslee et al. 2007). In addition to PINs, both PGP1/ABCB1 and PGP19/ABCB19 function in a transport mechanism that contributes to the patterning process during *Arabidopsis* embryo development (Mravec et al. 2008).

Also, correct membrane compartmentalization is important for correct cell polarity and PIN localization as seen in mutants defected in sterol synthesis (Willemsen et al. 2003), and recent data suggest that PGP19/ABCB19 stabilizes PIN1 localization at the plasma membrane (Titapiwatanakun et al. 2008). We do not know, however, if the NPA treatment of the young embryos caused any membrane damage.

NPA causes cotyledon fusion in developing somatic embryos

The most dramatic effect on the morphology of somatic embryos that we observed on embryos that had been exposed continuously to NPA during their whole maturation growth was on the outgrowth of cotyledons (Figure 2). By culturing different staged embryos on medium containing NPA, we found that the transition stage (i.e., pre-cotyledonary embryos, stage 2) was the stage most sensitive to the disturbance caused by NPA that leads to the abnormal cup-shaped form of cotyledons (Table 3; Figure 2C) or to the more severe pin-formed embryo morphology (Figure 2B and D). Our results indicate that after cotyledons are initiated, and with them the vascular patterning, the embryos appear to be less sensitive to NPA, and form almost normal-looking embryos with well-separated cotyledons, although they were more greenish and thicker than the cotyledons of the control embryos.

In gymnosperms the number of cotyledons varies greatly between species, and also within the species; for example, *Taxus* has 2 cotyledons; *Pinus* has 4–15 (20–23 in *P. maximartinezii*) and *Picea* has 4–15 cotyledons (Vidakovic 1991). Different numbers of cotyledons can also be formed on *P. abies* somatic embryos that are derived from the same cell line, which implicates the role of the culture conditions apart from the genetic background. The cotyledons are usually formed in a single whorl at the shoot apex (Figure 1F and H), but sometimes cotyledons are initiated from several circlets at the apex of somatic embryos, which is often more commonly seen in certain cell lines (Hakman, unpublished). The high number of cotyledons thus gives *Picea* somatic embryos their typical morphology, but after NPA treatment the embryos had defects of fused cotyledons that are similar to the defects commonly seen on angiosperm embryos after exposure to the chemical inhibitors of auxin transport, such as those in *B. juncea* (Liu et al. 1993, Hadfi et al. 1998), *Eleutherococcus senticosus* (Rupr. & Maxim.) Maxim. (Choi et al. 2001) and *Panax ginseng* Rzed. (Choi et al. 1997). This suggests a common mechanism behind cotyledon formation within the species of angiosperms and conifers, despite their cotyledon number which normally differ (for further discussion of cotyledon organogenesis see also review by Chandler 2008). In addition, the *polycotyledon* mutant of tomato has enhanced polar auxin transport suggesting a link between the phenotype and the auxin distribution (Al-Hammadi et al. 2003).

Genes that are involved in auxin perception and transduction and in auxin transport, such as the auxin efflux carrier gene *PIN1*, have been shown to participate in embryo axis formation and in the formation and separation of cotyledon primordia (see e.g., review by Berleth and Chatfield 2002). In *Arabidopsis* the combination of *pin1* with *cuc1*, *cuc2* and *stm* background enhanced the *pin1* phenotype and resulted in embryos and seedlings with completely fused cup-shaped cotyledons that sometimes also lacked a SAM

(Aida et al. 2002). The genes, *STM* and the *CUP-SHAPED COTYLEDON 1* and *2* (*CUC1* and *2*), seem to be involved in the separation of the cotyledon primordia (Aida et al. 1999, Takada et al. 2001), and in a model put forward by Aida et al. (2002) *PIN1* and *MP* are suggested to regulate apical patterning partially through the control of *CUC* expression. The process of cotyledon formation also appears to share many similarities with the formation of leaf primordia, with auxin flux being controlled by PIN1 in the surface cells (Jenik et al. 2007). Local application of auxin and NPA onto cultured tomato shoot apices caused collar-shaped primordia encircling the entire apex or pin-like phenotypes, respectively (Reinhardt et al. 2000). The high local auxin concentration in the *P. abies* embryo epidermal cell layer (Figure 4) together with its high expression of the *PIN1*-like gene (Palovaara et al. unpublished) suggests this region to have an NPA-sensitive auxin transport leading to the aberrant cotyledons phenotype seen after NPA treatment (Table 2; Figures 2 and 4).

NPA causes broader procambium and RAM in developing somatic embryos

The expression of the *PIN1*-like gene was higher in embryos exposed to NPA than in the control embryos (Table 4). The vascular tissue also appeared to be more expanded in the NPA-treated embryos (Figure 4), but if such cells also became properly aligned and functional was, however, not determined. Vascular overgrowth is a common response to NPA, in a similar fashion to the mutant *pin1* phenotype in *Arabidopsis* (Mattsson et al. 1999, Wenzel et al. 2008). An increase in *PIN1*-like expression was also seen in the NPA-treated seedlings of *Arabidopsis* in which case the normal vascular PIN localization also expanded to the cortical cells of root tips treated with the inhibitors of polar auxin transport (Peer et al. 2004, Vieten et al. 2005). As noted earlier, NPA acts by inhibiting auxin efflux from cells, which then, as a consequence, leads to auxin accumulation in treated cells (Petrásek et al. 2003). Auxin can modulate the transcription of *PIN1* through the TIR1-Aux/IAA-ARF pathway in *Arabidopsis* (Vieten et al. 2005) and, taken together, our results indicate that auxin regulates *P. abies PIN1*-like expression in a similar manner.

Clear auxin maxima in embryo roots could not be inferred from the immunolocalization analysis that are performed in this study, although the mature root tips stained intensively (Figure 5A). No clear difference in the staining intensity or in the staining pattern of IAA could be seen between embryos that had been treated with NPA and the control. However, the staining intensity was the highest in the early staged embryos and decreased as embryos matured, which is in agreement with IAA measurement of developing pine seeds (Sandberg et al. 1987). Recently, Larsson et al. (2008) also found that NPA treatment of the early staged *P. abies* somatic embryos (roughly corresponding to stage 1 embryos in this study) caused increased endogenous IAA concentration. An auxin imbalance in embryo axis then probably caused the broadening of both the procambium and the RAM that was seen in the NPA-treated embryos.

Conclusion

Our results show that NPA is harmful to early staged somatic embryos of *P. abies*, and that it causes cotyledon fusion and broadening of the RAM of precotyledonary embryos. For proper cotyledon initiation, correct auxin transport is needed only during a short period at the transition stage of embryo development, which is consistent with the results on *B. junceae* embryos (Liu et al. 1993). The defect of fused cotyledons seen on the developing embryos is similar to that commonly seen on angiosperm embryos after exposure to the chemical inhibitors of auxin transport. Our results also show that a *PIN1*-like gene is expressed during the earliest stages of somatic embryo development, confirming the importance of polar auxin transport during these stages. In addition, there is a drastic increase of *PIN* expression in the precotyledonary (stage 2) embryos treated with NPA compared to the untreated control embryos, which also is consistent with the earlier observations in *Arabidopsis* of how the inhibitors of auxin transport can modulate *PIN* gene expression in a way similar to that observed in *pin* mutants.

Supplementary Data

Supplementary data for this article are available at *Tree Physiology* Online.

Acknowledgment

The support from the University of Kalmar is gratefully acknowledged.

References

Aida, M., T. Ishida and M. Tasaka. 1999. Shoot apical meristem and cotyledon formation during *Arabidopsis* embryogenesis: interaction among the *CUP-SHAPED COTYLEDON* and *SHOOT MERISTEMLESS* genes. Development 126: 1563–1570.

Aida, M., T. Vernoux, M. Furutani, J. Traas and M. Tasaka. 2002. Roles of PIN-FORMED1 and MONOPTEROS in pattern formation of the apical region of the *Arabidopsis* embryo. Development 129:3965–3974.

Al-Hammadi, A.S.A., Y. Sreelakshmi, S. Negi, I. Siddiqi and R. Sharma. 2003. The *polycotyledon* mutant of tomato shows enhanced polar auxin transport. Plant Physiol. 133: 113–125.

Attree, S.M. and L.C. Fowke. 1995. Conifer somatic embryogenesis, embryo development, maturation drying and plant formation. *In* Plant Cell, Tissue and Organ Culture – Fundamental Methods. Eds. O.L. Gamborg and

G.C. Phillips. Springer-Verlag, Berlin/Heidelberg/New York, pp 103–113.

Avsian-Kretchmer, O., J.-C. Cheng, L. Chen, E. Moctezuma and Z.R. Sung. 2002. Indole acetic acid distribution coincides with vascular differentiation pattern during *Arabidopsis* leaf ontogeny. Plant Physiol. 130:199–209.

Bailly, A., V. Sovero, V. Vincenzetti, D. Santelia, D. Bartnik, B.W. Koenig, S. Mancuso, E. Martinoia and M. Geisler. 2008. Modulation of P-glycoproteins by auxin transport inhibitor is mediated by interaction with immunophilins. J. Biol. Chem. 283:21817–21826.

Benková, E., M. Michniewicz, M. Sauer, T. Teichmann, D. Seifertová, G. Jürgens and J. Friml. 2003. Local, efflux-dependent auxin gradients as a common module for plant organ formation. Cell 115:591–602.

Berleth, T. and S. Chatfield. 2002. Embryogenesis: pattern formation from a single cell. *In* The *Arabidopsis* Book. American Society of Plant Biologists.

Blakeslee, J.J., A. Bandyopadhyay, O.R. Lee et al. 2007. Interactions among PIN-FORMED and P-glycoprotein auxin transporters in *Arabidopsis*. Plant Cell 19:131–147.

Breuninger, H., E. Rikirsch, M. Hermann, M. Ueda and T. Laux. 2008. Differential expression of WOX genes mediates apical–basal axis formation in the *Arabidopsis* embryo. Dev. Cell 14:867–876.

Caruso, J.L., V.C. Pence and L.A. Leverone. 1995. Immunoassay methods of plant hormone analysis. *In* Plant Hormones, Physiology, Biochemistry and Molecular Biology. Ed. P.J. Davies. Kluwer, Dordrecht, pp 433–447.

Chandler, J.W. 2008. Cotyledon organogenesis. J. Exp. Bot. 59:2917–2931.

Choi, Y.E., H.S. Kim, W.Y. Soh and D.C. Yang. 1997. Developmental and structural aspects of somatic embryos formed on medium containing 2,3,5-triiodobenzoic acid. Plant Cell Rep. 16:738–744.

Choi, Y.E., M. Katsumi and H. Sano. 2001. Triiodobenzoic acid, an auxin polar transport inhibitor, suppresses somatic embryos formation and postembryonic shoot/root development in *Eleutherococcus senticosus*. Plant Sci. 160: 1183–1190.

Dhonukshe, P., I. Grigoriev, R. Fischer et al. 2008. Auxin transport inhibitors impair vesicle motility and actin cytoskeleton dynamics in diverse eukaryotes. Proc. Natl. Acad. Sci. USA 105:4489–4494.

Fischer-Iglesias, C., B. Sundberg, G. Neuhaus and A.M. Jones. 2001. Auxin distribution and transport during embryonic pattern formation in wheat. Plant J. 26:115–129.

Friml, J., E. Benková, I. Blilou et al. 2002. At PIN4 mediates sink-driven auxin gradients and root patterning in *Arabidopsis*. Cell 108:661–673.

Friml, J., A. Vieten, M. Sauer, D. Weijers, H. Schwarz, T. Hamann, R. Offringa and G. Jürgens. 2003. Efflux-dependent auxin gradients establish the apical–basal axis of *Arabidopsis*. Nature 426:147–153.

Furutani, M., T. Vernoux, J. Traas, T. Kato, M. Tasaka and M. Aida. 2004. PIN-FORMED1 and PINOID regulate boundary formation and cotyledon development in *Arabidopsis* embryogenesis. Development 131:5021–5030.

Gälweiler, L., C. Guan, A. Muller, E. Wisman, K. Mendgen, A. Yephremov and K. Palme. 1998. Regulation of polar auxin transport by AtPIN1 in *Arabidopsis* vascular tissue. Science 282:2226–2230.

Geldner, N., J. Friml, Y.-D. Stierhof, G. Jürgens and K. Palme. 2001. Auxin transport inhibitors block PIN1 cycling and vesicle trafficking. Nature 413:425–428.

Gorbatenko, O. and I. Hakman. 1995. The effect of Brefeldin A on the Golgi apparatus in Norway spruce cells. *In* Current Issues in Plant Molecular and Cellular Biology – Proceedings of the VIIIth International Congress on Plant Tissue and Cell Culture, Florence, Italy, 12–17 June, 1994. Eds. M. Terzi, R. Cella and A. Falavigna. Kluwer Academic Publishers, pp 633–638.

Grieneisen, V.A., J. Xu, A.F. Marée, P. Hogeweg and B. Scheres. 2007. Auxin transport is sufficient to generate a maximum and gradient guiding root growth. Nature 449:1008–1013.

Hadfi, K., V. Speth and G. Neuhaus. 1998. Auxin-induced developmental patterns in *Brassica juncea* embryos. Development 125:879–887.

Haecker, A., R. Gross-Hardt, B. Geiges, A. Sarkar, H. Breuninger, M. Herrmann and T. Laux. 2004. Expression dynamics of WOX genes mark cell fate decisions during early embryonic patterning in *Arabidopsis thaliana*. Development 131:657–668.

Hakman, I., L.C. Fowke, S. von Arnold and T. Eriksson. 1985. The development of somatic embryos in tissue cultures initiated from immature embryos of *Picea abies* (Norway spruce). Plant Sci. 38:53–59.

Hakman, I., P.J. Rennie and L.C. Fowke. 1987. A light and electron microscope study of *Picea glauca* (White spruce) somatic embryos. Protoplasma 140:100–109.

Jenik, P.D. and M.K. Barton. 2005. Surge and destroy: the role of auxin in plant embryogenesis. Development 132:3577–3585.

Jenik, P.D., C.S. Gillmor and W. Lukowitz. 2007. Embryonic patterning in *Arabidopsis thaliana*. Annu. Rev. Cell Dev. Biol. 23:207–236.

Katekar, G.F. and A.E. Geissler. 1980. Auxin transport inhibitors. IV. Evidence of common mode of action for proposed class of auxin transport inhibitors: the phytotropins. Plant Physiol. 66:1190–1195.

Kramer, E.M. 2008. Computer models of auxin transport: a review and commentary. J. Exp. Bot. 59:45–53.

Larsson, E., F. Sitbon, K. Ljung and S. von Arnold. 2008. Inhibited polar auxin transport results in aberrant embryo development in Norway spruce. New Phytol. 177:356–366.

Leverone, L.A., T.L. Stroup and J.L Caruso. 1991. Western blot analysis of cereal grain prolamines using an antibody to carboxyl-linked indole acetic acid. Plant Physiol. 96: 1076–1078.

Liu, C.-M., Z.-H. Xu and N.-H. Chua. 1993. Auxin polar transport is essential for the establishment of bilateral symmetry during early plant embryogenesis. Plant Cell 5:621–630.

Maisch, J. and P. Nick. 2007. Actin is involved in auxin-dependent patterning. Plant Physiol. 143:1695–1704.

Mattsson, J., Z.R. Sung and T. Berleth. 1999. Response of vascular systems to auxin transport inhibition. Development 126:2979–2991.

Moctezuma, E. 1999. Changes in auxin patterns in developing gynophores of the peanut plant (*Arachis hypogaea* L.). Ann. Bot. 83:235–242.

Mravec, J., M. Kubeš, A. Bielach, V. Gaykova, J. Petrásek, P. Skupa, S. Chand, E. Benková, E. Zazímalová and J. Friml. 2008. Interaction of PIN and PGP transport mechanisms in

auxin distribution-dependent development. Development 135: 3345–3354.

Murphy, A.S., K.R. Hoogner, W.A. Peer and L. Taiz. 2002. Identification, purification, and molecular cloning of N-1-naphthylphthalamic acid-binding plasma membrane-associated aminopeptidase from *Arabidopsis*. Plant Physiol. 128:935–950.

Nagashima, A., Y. Uehara and T. Sakai. 2008. The ABC subfamily B auxin transporter AtABCB19 is involved in the inhibitory effects of *N*-1-naphthylphthalamic acid on the phototropic and gravitropic responses of *Arabidopsis* hypocotyls. Plant Cell Physiol. 49:1250–1255.

Nawy, T., W. Lukowitz and M. Bayer. 2008. Talk global, act local-patterning the *Arabidopsis* embryo. Curr. Opin. Plant Biol. 11:28–33.

Noh, B., A.S. Murphy and E.P. Spalding. 2001. *Multidrug Resistance*-like genes of *Arabidopsis* required for auxin transport and auxin-mediated development. Plant Cell 13: 2441–2454.

Okada, K., J. Ueda, M.K. Komaki, C.J. Bell and Y. Shimura. 1991. Requirement of the auxin polar transport system in early stages of *Arabidopsis* floral bud formation. Plant Cell 3:677–684.

Palovaara, J. and I. Hakman. 2008. Conifer WOX-related homeodomain transcription factors, developmental consideration and expression dynamic of WOX2 during *Picea abies* somatic embryogenesis. Plant Mol. Biol. 66: 533–549.

Peer, W.A., A. Bandyopadhyay, J.J. Blakeslee, S.N. Makam, R.J. Chen, P.H. Masson and A.S. Murphy. 2004. Variation in expression and protein localization of the PIN family of auxin efflux facilitator proteins in flavonoid mutants with altered auxin transport in *Arabidopsis thaliana*. Plant Cell 16: 1898–1911.

Petrásek, J., A. Cerná, K. Schwarzerová, M. Elckner, D.A. Morris and E. Zazímalová. 2003. Do phytotropins inhibit auxin efflux by impairing vesicle traffic? Plant Physiol. 131:254–263.

Petrásek, J., J. Mravec, R. Bouchard et al. 2006. PIN proteins perform a rate-limiting function in cellular auxin efflux. Science 312:914–918.

Raghavan, V. and K.K. Sharma. 1995. Zygotic embryogenesis in gymnosperms and angiosperms. *In In Vitro* Embryogenesis in Plants. Current Plant Science and Biotechnology in Agriculture Volume 20. Ed. T.A. Thorpe. Kluwer Academic Publisher, pp 73–115.

Rahman, A., A. Bannigan, W. Sulaman, P. Pechter, E.B. Blancaflor and T.I. Baskin. 2007. Auxin, actin and growth of the *Arabidopsis thaliana* primary root. Plant J. 50:514–528.

Reinhardt, D., T. Mandel and C. Kuhlemeier. 2000. Auxin regulates the initiation and radial position of plant lateral organs. Plant Cell 12:507–518.

Sandberg, G., A. Ernstsen and M. Hamnede. 1987. Dynamics of indole-3-acetic acid and indole-3-ethanol during development and germination of *Pinus sylvestris* seeds. Physiol. Plant. 71:411–418.

Schiavone, F.M. 1988. Micromanipulation of somatic embryos of the domesticated carrot reveals apical control of axis elongation and root regeneration. Development 103:657–664.

Singh, H. 1978. Embryology of gymnosperms. Encyclopedia of plant anatomy. Gebrüder Borntraaeger. Berlin, Stuttgart, pp 302.

Spurr, A.R. 1949. Histogenesis and organization of the embryo in *Pinus strobus* L. Am. J. Botany 36:629–641.

Steinmann, T., N. Geldner, M. Grebe, S. Mangold, C.L. Jackson, S. Paris, L. Gälweiler, K. Palme and G. Jürgens. 1999. Coordinated polar localization of auxin efflux carrier PIN1 by GNOM ARF GEF. Science 286:316–318.

Swarup, R., A. Marchant and M.J. Bennett. 2000. Auxin transport: providing a sense of direction during plant development. Biochem. Soc. Trans. 28:481–485.

Takada, S., K. Hibara, T. Ishida and M. Tasaka. 2001. The CUP-SHAPED COTYLEDON1 gene of *Arabidopsis* regulates shoot apical meristem formation. Development 128:1127–1135.

Tanaka, H., P. Dhonukshe, P.B. Brewer and J. Friml. 2006. Spatiotemporal asymmetric auxin distribution: a means to coordinate plant development. Cell. Mol. Life Sci. 63:2738–2754.

Titapiwatanakun, B. and A.S. Murphy. 2008. Post-transcriptional regulation of auxin transport proteins: cellular trafficking, protein phosphorylation, protein maturation, ubiquitination, and membrane composition. J. Exp. Bot. doi:10.1093/jxb/ern240.

Titapiwatanakun, B., J.J. Blakeslee and A. Bandyopadhyay et al. 2008. ABCB19/PGP19 stabilises PIN1 in membrane microdomains in *Arabidopsis*. Plant J. doi: 10.1111/j.1365-313X.2008.03668.x.

Verrier, P.J., D. Bird, B. Burla et al. 2008. Plant ABC proteins – a unified nomenclature and updated inventory. Trends Plant Sci. 13:151–159.

Vidakovic, M. 1991. Conifers: morphology and variations Graficki Zavod Hrvatske, Croatia, 754 p.

Vieten, A., S. Vanneste, J. Wisniewska, E. Benková, R. Benjamins, R., T. Beeckman, C. Luschnig and J. Friml. 2005. Functional redundancy of PIN proteins is accompanied by auxin-dependent cross-regulation of PIN expression. Development 132:4521–4531.

Walker, N.J. 2002. A technique whose time has come. Science 269:257–259.

Weijers, D. and G. Jürgens. 2005. Auxin and embryo axis formation: the ends in sight? Curr. Opin. Plant Biol. 8: 32–37.

Weijers, D., M. Sauer, O. Meurette, J. Friml, K. Ljung, G. Sandberg, P. Hooykaas and R. Offringa. 2005. Maintenance of embryonic auxin distribution for apical–basal patterning by PIN-FORMED–dependent auxin transport in *Arabidopsis*. Plant Cell 17:2517–2526.

Wenzel, C.L., Q. Hester and J. Mattsson. 2008. Identification of genes expressed in vascular tissues using NPA-induced vascular overgrowth in *Arabidopsis*. Plant Cell Physiol. 49:457–468.

Willemsen, V., J. Friml, M. Grebe, A. van den Toorn, K. Palme and B. Scheres. 2003. Cell polarity and PIN protein positioning in *Arabidopsis* require STEROL METHYLTRANSFER ASE1 function. Plant Cell 15:612–625.